

Proceeding

# Harsh Environmental Surface Acoustic Wave Temperature Sensor Based on Pure and Scandium doped Aluminum Nitride on Sapphire <sup>†</sup>

Manuel Gillinger, Theresia Knobloch, Michael Schneider and Ulrich Schmid

Institute of Sensor and Actuator Systems, TU Wien, Vienna 1040, Austria

<sup>†</sup> Presented at the Eurosensors 2017 Conference, Paris, France, 3–6 September 2017.

Published: 17 August 2017

**Abstract:** This paper investigates the performance of surface acoustic wave (SAW) devices as low power MEMS temperature sensors using reactive sputter deposited aluminum nitride (AlN) and scandium doped aluminum nitride (AlScN) as piezoelectric layers on sapphire substrates. In detail, devices with a wavelength of 16  $\mu\text{m}$  are fabricated with both AlN and AlScN films having a resonance frequency at room temperature of  $\sim 354$  MHz and  $\sim 349$  MHz, respectively. The samples are placed in a furnace and measured in argon atmosphere up to 800 °C. The temperature dependency on the frequency shows for both materials a linear decrease up to the maximum measured temperature level resulting in constant temperature coefficients of  $-27.62$  kHz/°C and  $-27.81$  kHz/°C, respectively.

**Keywords:** AlN; AlScN; SAW; harsh environmental; high temperature

## 1. Introduction

Surface acoustic wave (SAW) devices have been key components in telecommunication systems for the last decades [1]. The optimal choice of piezoelectric material is one of the main challenges to realize such sensors. Currently, commercially available SAW devices are based on langasite ( $\text{La}_3\text{Ga}_5\text{SiO}_{14}$ , LGS), langatate ( $\text{La}_3\text{Ga}_{5.5}\text{Ta}_{0.5}\text{O}_{14}$ , LGT) or langanite ( $\text{La}_3\text{Ga}_{5.5}\text{Nb}_{0.5}\text{O}_{14}$ , LGN), whose major disadvantage is the low phase velocity (e.g., 2700 m/s in LGS) and high acoustic propagation losses during high temperature load [2–4]. Aluminum nitride (AlN) or scandium doped aluminum nitride (AlScN) on sapphire is regarded as a promising alternative to LGS, LGT and LGN, given much higher phase velocities  $v_p$  above 5600 m/s [5,6]. With these higher phase velocities, higher frequencies  $f_0$  can be achieved with the same device dimensions (at fixed wavelength  $\lambda$ ), due to the relation  $f_0 = \lambda/v_p$ . AlN promises operation up to 700°C even in pure oxygen atmosphere for two hours without measurable film degeneration [7]. Whereas, AlScN has a higher  $d_{33}$  and therefore the electro-mechanical coupling factor is increased by a factor of  $\sim 3$ , compared to pure AlN [8–10].

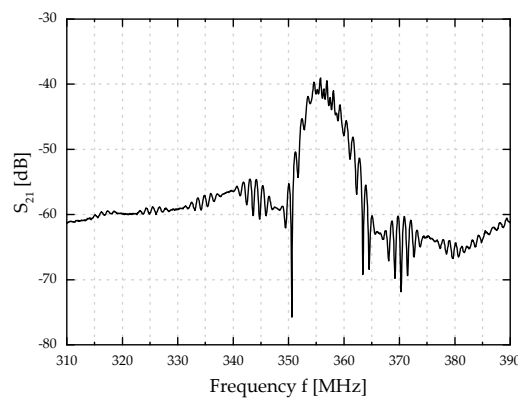
## 2. Experimental Details

The sapphire substrate is cleaned in pure argon plasma by an inverse sputter etch step, with a power of 500 W and a back pressure of 6  $\mu\text{bar}$  for 5 min, before depositing the piezoelectric thin film. A target cleaning step prior deposition is performed at closed shutter position. Afterwards, AlN is sputtered from an aluminum target ( $\varnothing$  150 mm, purity 5N) with a plasma power of 800 W at a back pressure of 2  $\mu\text{bar}$  in pure nitrogen gas (purity 6N) with a constant gas flow of 50 sccm. AlScN is sputtered from a scandium/aluminum alloy target (27<sub>at%</sub>/73<sub>at%</sub>,  $\varnothing$  100 mm) with a power of 400 W and a pressure of 4  $\mu\text{bar}$  in an argon/nitrogen gas atmosphere (30/20 sccm). The distance between target and substrate is fixed at 65 mm. The parameters were chosen based on pre-investigations for good c-axis orientation [7,11]. The total film thickness  $h$  is 2  $\mu\text{m}$ . Next, inter-digital transducers (IDTs) using a bilayer of 5 nm tantalum and 40 nm platinum as robust electrode material are patterned using a

standard lift-off process. The IDTs are aligned to ensure wave propagation parallel to the crystallographic  $a$ -direction ( $\langle 11\bar{2}0 \rangle$ ) of the sapphire substrate. The IDTs have 40 finger pairs with an aperture of  $1400\ \mu\text{m}$  and a wavelength  $\lambda$  of  $16\ \mu\text{m}$ , what results in a normalized thickness  $kh = 2\pi h/\lambda = 0.78$ . The distance between transmitter and receiver is  $4350\ \mu\text{m}$ . After fabrication, the devices are placed in a furnace and connected to a network vector analyzer from Rhode and Schwarz (ZVL6).  $S_{21}$ -parameters are measured starting at room temperature and in steps of about  $200\ ^\circ\text{C}$  up to  $812\ ^\circ\text{C}$ . At each temperature step, each device is measured 10 times by consecutively connecting and disconnecting the NVA to the samples. The sensitivity of the SAW devices is determined by measuring the shift of the resonance frequency during temperature load.

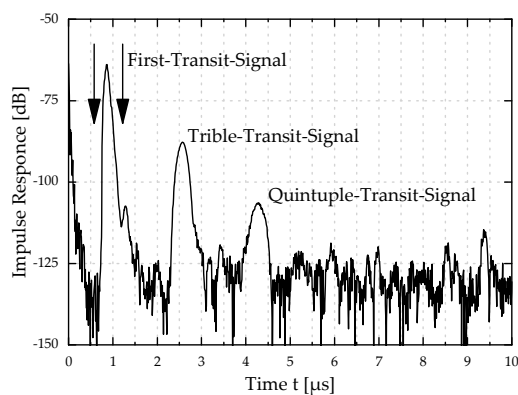
### 3. Results

Figure 1 shows a typical raw  $S_{21}$  characteristics of an AlN/sapphire delay line device with  $kh = 0.78$  and a transmitter receiver distance of  $4350\ \mu\text{m}$ . Delay line devices are basically band-pass filters, which show a minimum damping at the resonance frequency  $f_0$ .



**Figure 1.** Raw  $S_{21}$  measurement for  $kh = 0.78$  and a distance  $d = 4350\ \mu\text{m}$  between transmitter and receiver.

The corresponding impulse response from Figure 1 is shown in Figure 2. The two arrows define the gating window of the first impulse starting at  $0.87\ \mu\text{s}$  for filtering the SAW signal to eliminate parasitic crosstalk between transmitter and receiver. The impulse response also shows the triple-transit signal as well the quintuple transit signal at  $2.53\ \mu\text{s}$  and  $4.19\ \mu\text{s}$ , respectively. The damping increases by around 20 dB for subsequent higher order signals, which is attributed to both the wave damping in transit and the transducer losses.



**Figure 2.** Impulse response for  $kh = 0.78$ ; arrows indicate the gating window at the first peak.

Figure 3a shows selected gated  $S_{21}$  measurements for an AlN-based device between  $25\ ^\circ\text{C}$  and  $812\ ^\circ\text{C}$ . The resonance frequency  $f_0$  shifts to lower values at higher temperatures due to the thermally

induced expansion of the materials involved. The different peak height at  $f_0$  for each temperature is attributed to the varying contact resistance when manually re-contacting the SAW devices between each measurement step. A similar behavior is observed for the AlScN device, as illustrated in Figure 3b.

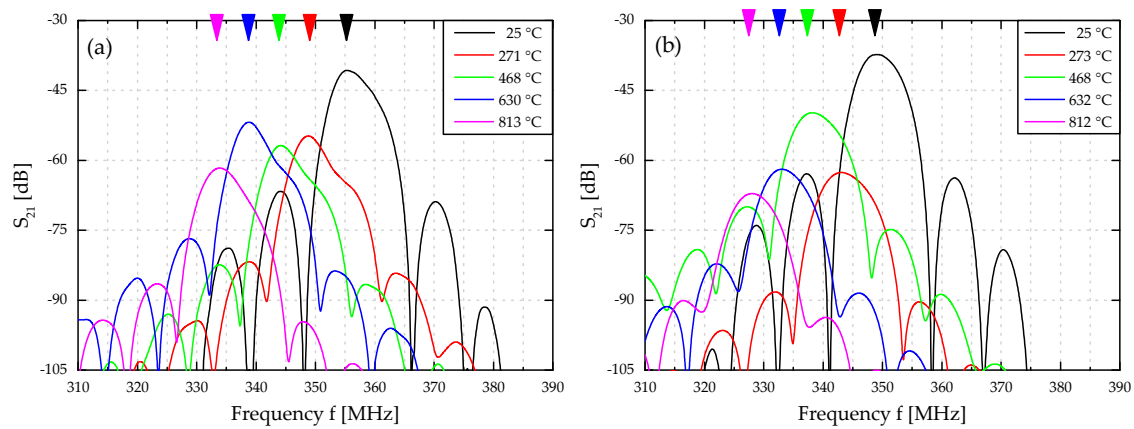


**Figure 3.** (a) Selected gated first impulse pure AlN (a) and AlScN (b) for operating temperatures up to 812 °C.

The temperature coefficient of frequency (TCF) is determined by plotting the evaluated resonance frequency  $f_0$  versus the measurement temperature. At room temperature, the devices feature resonance frequencies  $f_0 = 354.78$  MHz for AlN and  $f_0 = 349.22$  MHz for AlScN. The lower sound velocities for AlScN is due to a lower Young's modulus of the piezoelectric layer. For pure AlN, a TCF of  $-27.62$  kHz/°C and for AlScN a TCF of  $-27.81$  kHz/°C are evaluated, as shown in Figure 4.

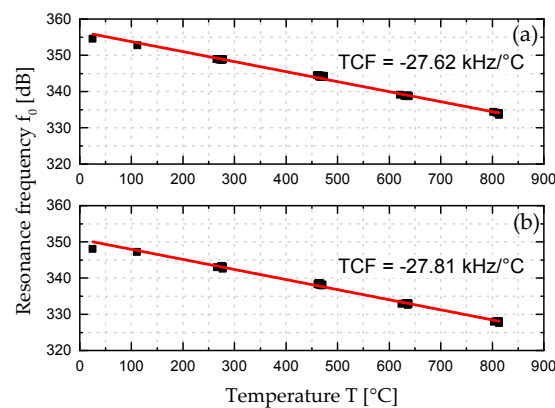


**Figure 4.** Temperature coefficient of frequency for AlN (a) and scandium doped AlN (b) on c-plane sapphire (10 measurement points at each temperature level).

#### 4. Conclusions

Compared to LGS devices with a TCF requesting the quadratic term to represent the temperature dependence [12], SAW devices based on AlN or AlScN on top of a sapphire substrate show a linear behavior giving the opportunity to realize a MEMS temperature sensor up to 812 °C with a constant TCF. Due to the different sound velocities, a slightly different resonance frequency for the same structure size is observed. Combined with an additional antenna element, key components are available to pave the way for robust wireless and battery less linear temperature sensor modules for harsh environmental applications.

**Acknowledgments:** This project has been supported within the COMET – Competence Centers for Excellent Technologies Programme by BMVIT, BMWFJ and the federal provinces of Carinthia and Styria. Many thanks go to Jochend Bardong at CTR Carinthian Tech Research, Villach, for providing the high temperature measurement equipment for SAW characterization.

**Conflicts of Interest:** The authors declare no conflict of interest.

## References

1. Macchiarella, G.; Stracca, G.B. SAW Devices for Telecommunications: Examples and Applications. In Proceedings of the 1982 Ultrasonics Symposium, San Diego, CA, USA, 27–29 October 1982.
2. Aubert, T.; Elmazria, O.; Assouar, M.B. Wireless and batteryless surface acoustic wave sensors for high temperature environments. In Proceedings of the 2009 9th International Conference on Electronic Measurement & Instruments, Beijing, China, 16–19 August 2009.
3. Fachberger, R.; Bruckner, G.; Hauser, R.; Biniasch, J.; Reindl, L.; Ruppel, C.C.W. Properties of radio frequency Rayleigh waves on langasite at elevated temperatures. In Proceedings of the IEEE Ultrasonics Symposium, 2004, Montreal, QC, Canada, 23–27 August 2004.
4. Cunha, M.P.d. Wireless sensing in hostile environments. In Proceedings of the 2013 IEEE International Ultrasonics Symposium (IUS), Prague, Czech Republic, 21–25 July 2013.
5. Gillinger, M.; Shaposhnikov, K.; Knobloch, T.; Schneider, M.; Kaltenbacher, M.; Schmid, U. Impact of layer and substrate properties on the surface acoustic wave velocity in scandium doped aluminum nitride based SAW devices on sapphire. *Appl. Phys. Lett.* **2016**, *108*, 231601.
6. Aubert, T.; Elmazria, O.; Assouar, B.; Hamdan, A.; Geneve, D. Reliability of AlN/sapphire bilayer structure for high-temperature SAW applications. In Proceedings of the 2010 IEEE International Ultrasonics Symposium, San Diego, CA, USA, 11–14 October 2010.
7. Gillinger, M.; Schneider, M.; Bittner, A.; Nicolay, P.; Schmid, U. Impact of annealing temperature on the mechanical and electrical properties of sputtered aluminum nitride thin films. *J. Appl. Phys.* **2015**, *117*, 065303.
8. Akiyama, M.; Kamohara, T.; Kano, K.; Teshigahara, A.; Takeuchi, Y.; Kawahara, N. Enhancement of Piezoelectric Response in Scandium Aluminum Nitride Alloy Thin Films Prepared by Dual Reactive Cosputtering. *Adv. Mater.* **2009**, *21*, 593–596, doi:10.1002/adma.200802611.
9. Mayrhofer, P.M.; Euchner, H.; Bittner, A.; Schmid, U. Circular test structure for the determination of piezoelectric constants of ScxAl1-xN thin films applying Laser Doppler Vibrometry and FEM simulations. *Sens. Actuators A Phys.* **2015**, *222*, 301–308.
10. Wang, W.; Mayrhofer, P.M.; He, X.; Gillinger, M.; Ye, Z.; Wang, X.; Bittner, A.; Schmid, U.; Luo, J.K. High performance AlScN thin film based surface acoustic wave devices with large electromechanical coupling coefficient. *Appl. Phys. Lett.* **2014**, *105*, 133502.
11. Mayrhofer, P.M.; Eisenmenger-Sittner, C.; Stöger-Pollach, M.; Euchner, H.; Bittner, A.; Schmid, U. The impact of argon admixture on the c-axis oriented growth of direct current magnetron sputtered ScxAl1-xN thin films. *J. Appl. Phys.* **2014**, *115*, 193505.
12. Aubert, T.; Elmazria, O.; Bardong, J.; Bruckner, G. Iridium interdigital transducers for ultra-high-temperature SAW devices, In Proceedings of the 2011 IEEE International Ultrasonics Symposium, Orlando, FL, USA, 18–21 October 2011.



© 2017 by the authors. Licensee MDPI, Basel, Switzerland. This article is an open access article distributed under the terms and conditions of the Creative Commons Attribution (CC BY) license (<http://creativecommons.org/licenses/by/4.0/>).